

Supplementary information

Theoretical Investigation of the Anchoring and Electrochemical
Performance of Transition Metal Carbides for Lithium–Sulfur
Batteries

Mingyang Wang^{1,2}, Jianjun Mao³ Yudong Pang¹, Xilin Zhang¹, Zongxian Yang^{1*}, Zhansheng Lu^{1*} and
Shuting Yang^{2,4*}

¹*School of Physics, Henan Normal University and Henan Key Laboratory of Photovoltaic Materials,
Xinxiang, Henan, 453007, People's Republic of China*

²*Henan Battery Research Institute, Xinxiang, Henan, 453007, People's Republic of China*

³*Department of Chemistry, The University of Hong Kong, Pok Fu Lam Road, Hong Kong, People's
Republic of China*

⁴*School of Chemistry and Chemical Engineering Science, Henan Normal University, Xinxiang, Henan
453007, People's Republic of China*

*Authors to whom correspondence should be addressed: yzx@htu.edu.cn (ZY); zslu@htu.edu.cn (ZL)

and yangshuting17@163.com (SY)

MODELS AND COMPUTATIONAL METHODS

In the present study, the (001) surface of six TMCs has been considered because it is the most stable one among the three

low-index Miller surfaces [1]. In addition, the (001) surface of TMCs have been widely applied in different research works [2-4]. The *ab initio* molecular dynamic (AIMD) simulation in the canonical (NVT) ensemble with the time step setting at 1 fs and temperature at 500 K for 10 ps was performed to test the thermal stability of (001) surface of TMCs. A (3×3) slabs surface with a vacuum layer of 20 Å along the *z*-direction to model the TMCs surface. During the electronic structure calculations, only the outmost two layers of the four layers were allowed to relax freely until the residual forces being less than 0.01 eV/Å. The adsorption energy (E_{ads}) of LiPSs on the substrate (TMCs) is defined as,

$$E_{ads} = E_{(LiPSs)} + E_{(TMC)} - E_{(LiPSs@TMC)} \quad (1)$$

where $E_{(LiPSs)}$, $E_{(TMC)}$, and $E_{(LiPSs@TMC)}$ are the total energies of LiPSs molecules, the pristine TMC (001) substrate, and the combined system of LiPSs on TMC substrate, respectively. With this definition, the positive binding energy indicates that the adsorption of LiPSs on the TMC substrate is energetically favorable. The ratio of vdW in the interactions between sulfur species and TMCs is computed using the following formula:

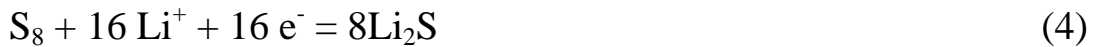
$$R = \frac{(E_{ads}^{vdW} - E_{ads}^{novdW})}{E_{ads}^{vdW}} \quad (2)$$

where E_{ads}^{vdW} and E_{ads}^{novdW} denote the binding energies of S₈/LiPSs with and without vdW interactions. So, the latter is defined as

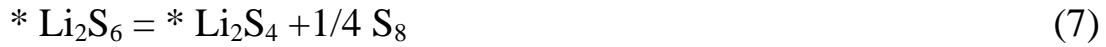
chemical interactions, and the difference between them is defined as vdW interactions. The charge transfer value (Δq) is defined as the difference of the number of electrons before and after interaction,

$$\Delta q = q_{\text{intrinsic}} - q_{\text{interaction}} \quad (3)$$

where $q_{\text{intrinsic}}$ and $q_{\text{interaction}}$ represent the number of electrons of a species before and after interaction, respectively. According to the definition, a positive Δq value represents lost of electrons and the negative value represents gain of electrons. The determination of the bonding and antibonding states between Li(S) and C(TM) atoms was obtained by the crystal orbital Hamilton population (COHP) as employed by the Lobster program[5-8]. The sulfur reduction reactions during the discharging processes of Li-S batteries are a 16-electron process with the formation of eight Li₂S molecules. The following are the details of the calculation of the Gibbs free energy for the each step of reduction of S₈ to Li₂S which are consisted with the previous work[9, 10].



The rudimentary steps involved in the generation of one Li₂S molecules are as follows,





wherein * represents an active site on the catalytic substrate.

The Gibbs free energy (ΔG) for each SRR step during the Li-S discharge process is calculated as

$$\Delta G = \Delta E + \Delta E_{ZPE} - T\Delta S \quad (10)$$

where ΔE is the DFT-computed energy difference between products and reactants, ΔE_{ZPE} is the contributions of zero-point energy and ΔS is entropy to the free energy, respectively.

FIGURES

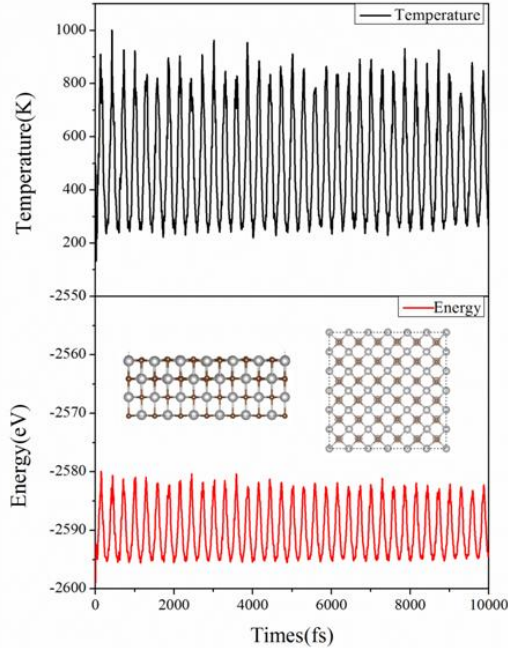


Fig. S1. The AIMD simulations at the temperature of 500 K lasting for 10 ps on the TiC(001) surface. The insert figures are the side and top views of the TiC(001) surface at the end of simulated time.

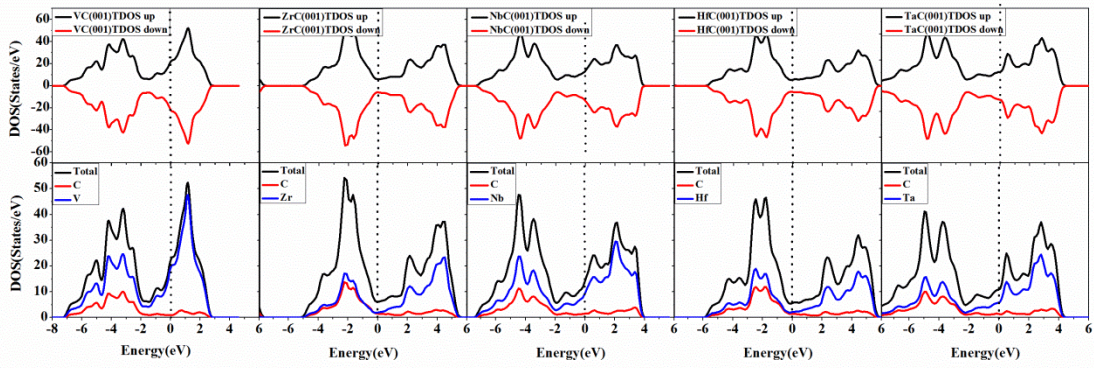


Fig. S2. The total and partial density of states of VC, ZrC, NbC, HfC, and TaC (001) surfaces.

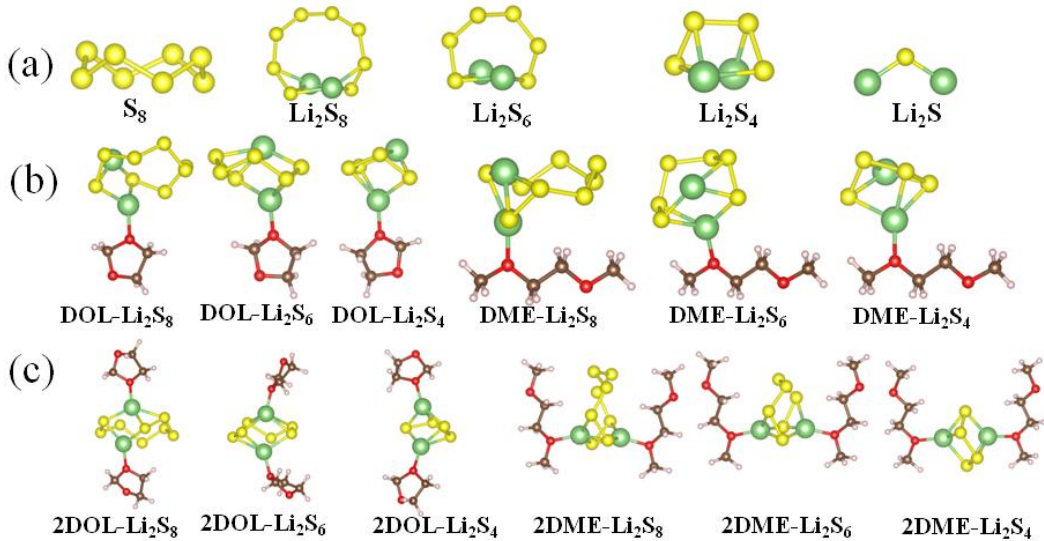


Figure S3. (a) The structures of S_8 and LiPSs; (b) The optimized adsorption structures of Li_2S_8 , Li_2S_6 , Li_2S_4 with DOL and DME, respectively; (c) The optimized adsorption structures of Li_2S_8 , Li_2S_6 , Li_2S_4 with two DOLs and two DMEs, respectively.

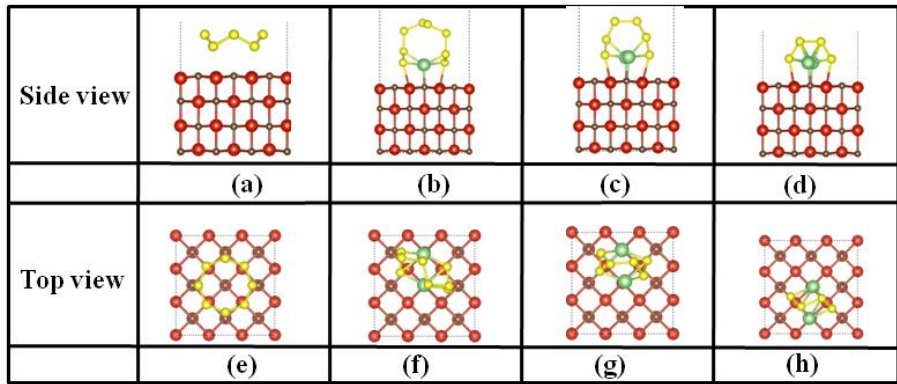


Fig. S4. The top and side views of the optimized adsorption structures of (a) and (e) S_8 , (b) and (f) Li_2S_8 , (c) and (g) Li_2S_6 , (d) and (h) Li_2S_4 , on $VC(001)$ surface, respectively.

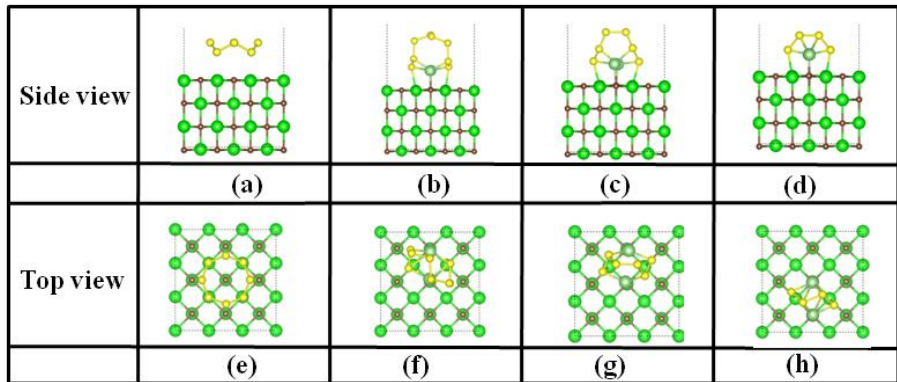


Fig. S5. The top and side views of the optimized adsorption structures of (a) and (e) S_8 , (b) and (f) Li_2S_8 , (c) and (g) Li_2S_6 , (d) and (h) Li_2S_4 , on $ZrC(001)$ surface, respectively.

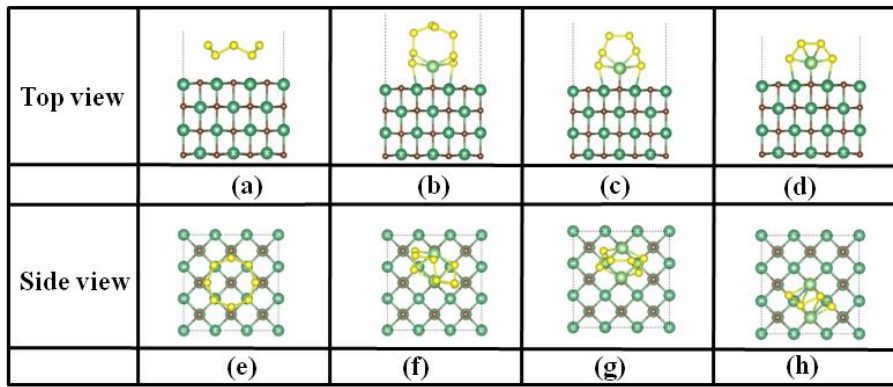


Fig. S6. The top and side views of the optimized adsorption structures of (a) and (e) S_8 , (b) and (f) Li_2S_8 , (c) and (g) Li_2S_6 , (d) and (h) Li_2S_4 , on $\text{NbC}(001)$ surface, respectively.

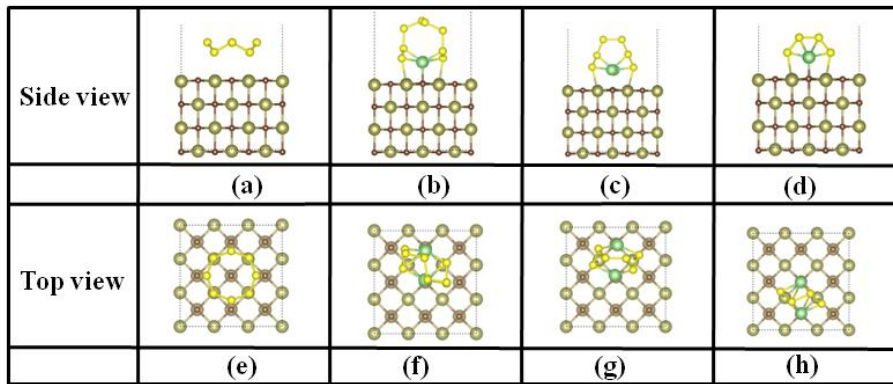


Fig. S7. The top and side views of the optimized adsorption structures of (a) and (e) S_8 , (b) and (f) Li_2S_8 , (c) and (g) Li_2S_6 , (d) and (h) Li_2S_4 , on $\text{HfC}(001)$ surface, respectively.

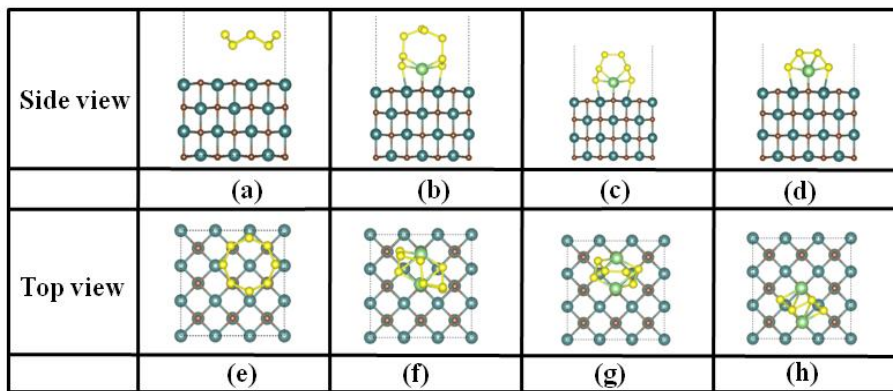


Fig. S8. The top and side views of the optimized adsorption structures of (a) and (e) S₈, (b) and (f) Li₂S₈, (c) and (g) Li₂S₆, (d) and (h) Li₂S₄, on TaC(001) surface, respectively.

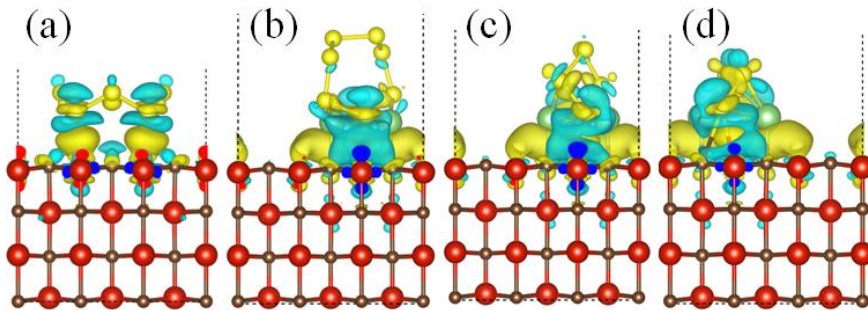


Fig. S9. Side views of CDD for (a) S₈, (b) Li₂S₈, (c) Li₂S₆, and (d) Li₂S₄ on VC. Yellow and blue regions indicate charge accumulation and charge depletion, respectively.

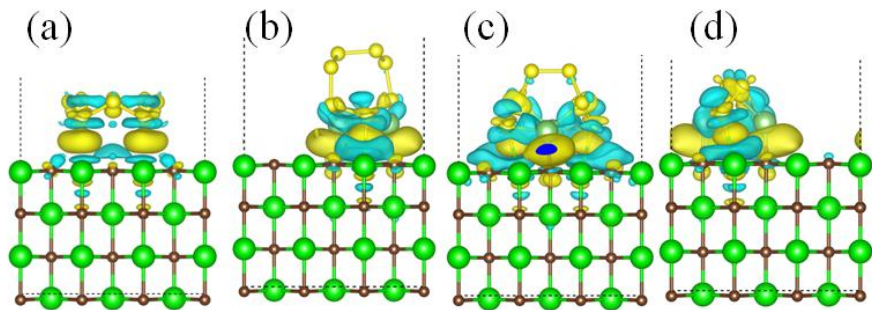


Fig. S10. Side views of CDD for (a) S_8 , (b) Li_2S_8 , (c) Li_2S_6 , and (d) Li_2S_4 on ZrC.

Yellow and blue regions indicate charge accumulation and charge depletion, respectively.

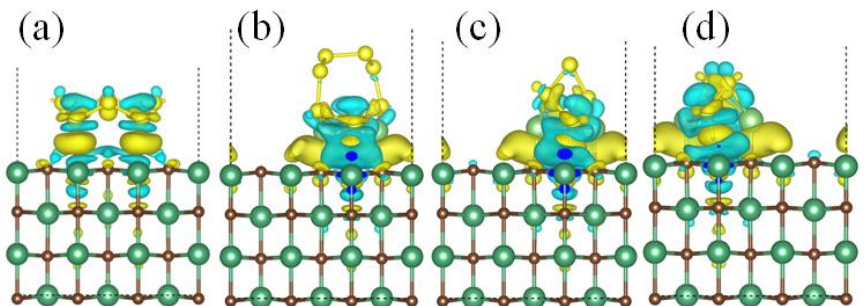


Fig. S11. Side views of CDD for (a) S_8 , (b) Li_2S_8 , (c) Li_2S_6 , and (d) Li_2S_4 on NbC.

Yellow and blue regions indicate charge accumulation and charge depletion, respectively.

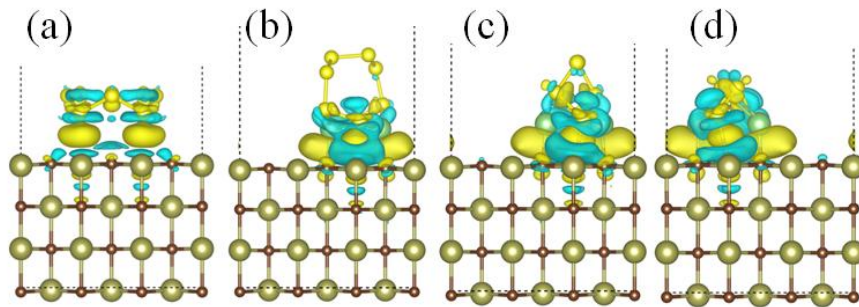


Fig. S12. Side views of CDD for (a) S_8 , (b) Li_2S_8 , (c) Li_2S_6 , and (d) Li_2S_4 on HfC.

Yellow and blue regions indicate charge accumulation and charge depletion, respectively.

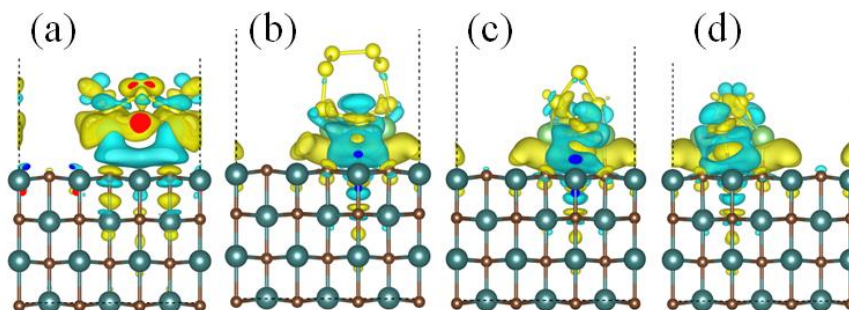


Fig. S13. Side views of CDD for (a) S_8 , (b) Li_2S_8 , (c) Li_2S_6 , and (d) Li_2S_4 on TaC.

Yellow and blue regions indicate charge accumulation and charge depletion, respectively.

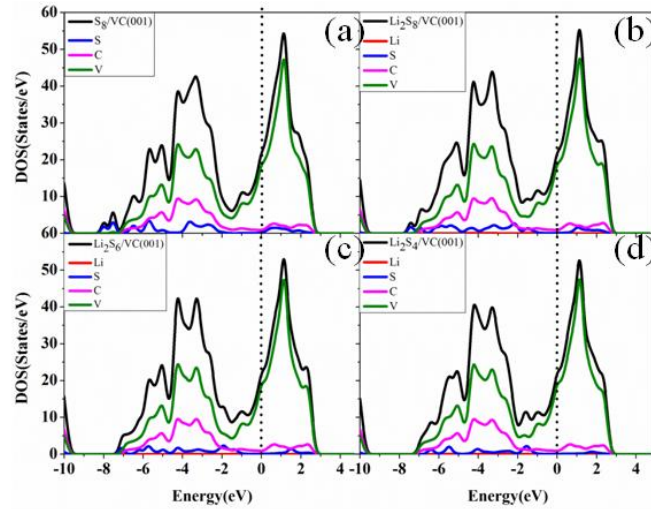


Fig. S14. The total and projected density of states of S_8 (a), Li_2S_8 (b), Li_2S_6 (c), and Li_2S_4 (d) on the $VC(001)$ surface, respectively.

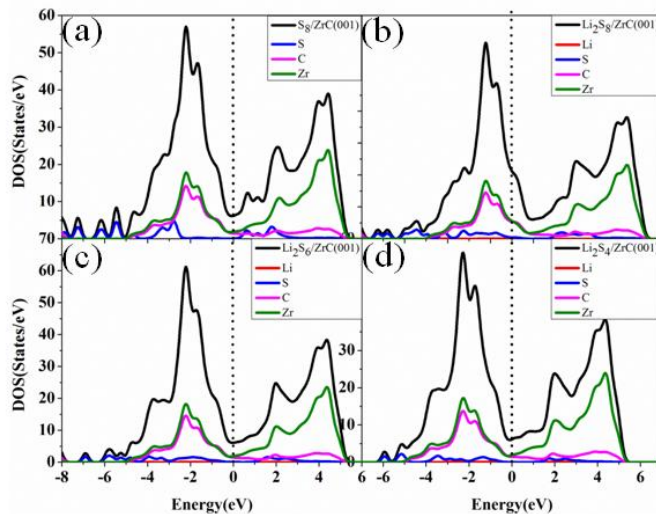


Fig. S15. The total and projected density of states of S_8 (a), Li_2S_8 (b), Li_2S_6 (c), and Li_2S_4 (d) on the $ZrC(001)$ surface, respectively.

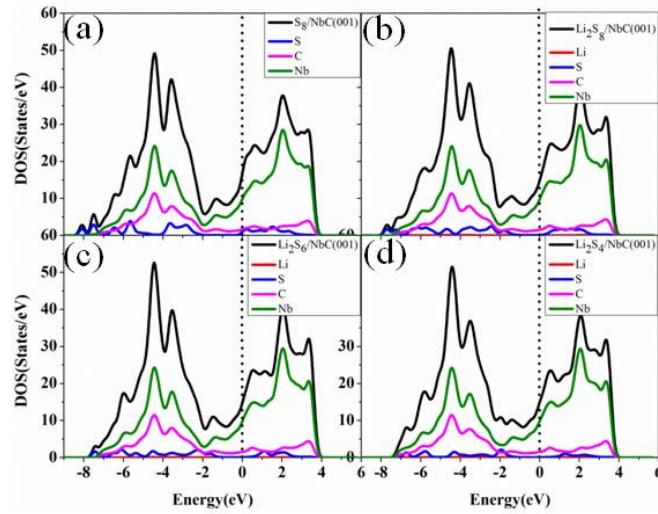


Fig. S16. The total and projected density of states of S_8 (a), Li_2S_8 (b), Li_2S_6 (c), and Li_2S_4 (d) on the $NbC(001)$ surface, respectively.

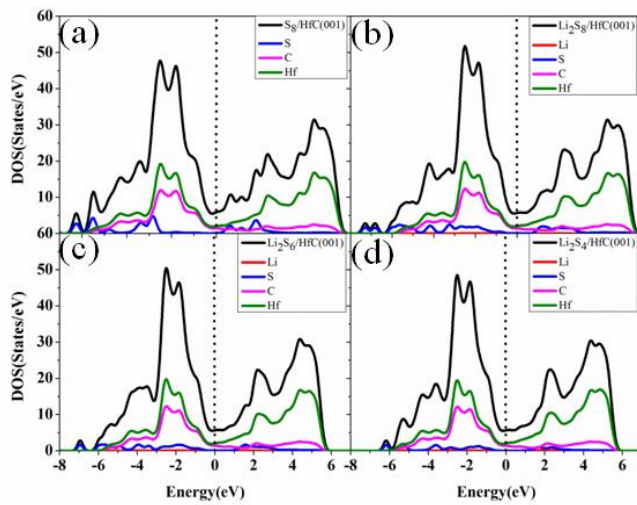


Fig. S17. The total and projected density of states of S_8 (a), Li_2S_8 (b), Li_2S_6 (c), and Li_2S_4 (d) on the $HfC(001)$ surface, respectively.

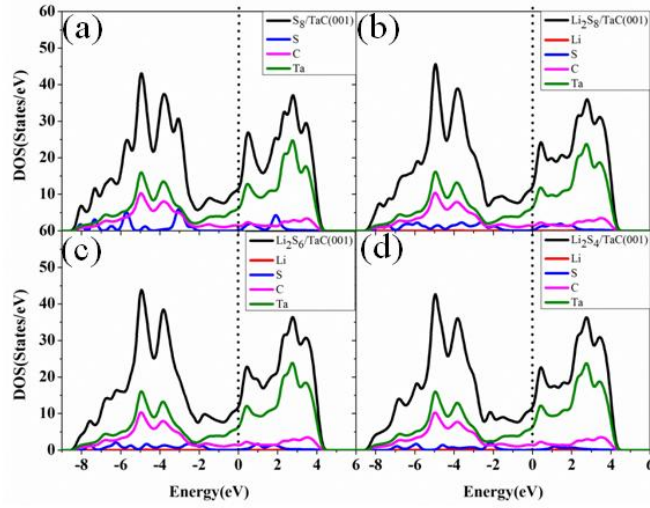


Fig. S18. The total and projected density of states of S_8 (a), Li_2S_8 (b), Li_2S_6 (c), Li_2S_4 (d) on TaC(001) surface, respectively.

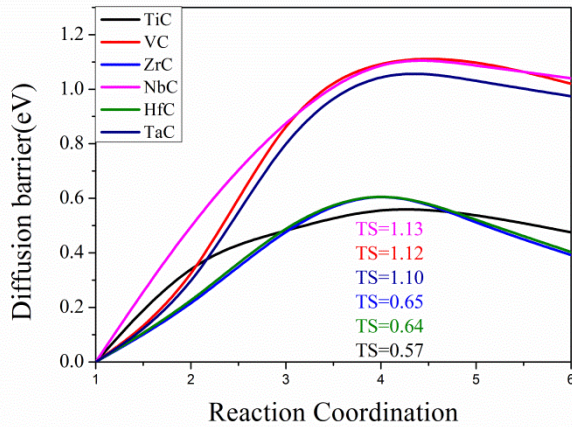


Fig. S19. The calculated minimum energy path of Li_2S decomposition on TMCs surfaces. The barriers' values are shown in the figure.

TABLES

Table S1. The lattice constants of TMCs and bond lengths of metal (C)-C(metal) of TMCs(001) surface.

	Lattice constant(Å)	The bond length of Metal-C (Å)	The bond length of Metal-metal (Å)	The bond length of C-C (Å)
TiC	4.333	2.170	3.063	3.063
VC	4.155	2.084	2.938	2.938
ZrC	4.710	2.356	3.330	3.330
NbC	4.506	2.259	3.186	3.186
HfC	4.647	2.325	3.286	3.286
TaC	4.478	2.247	3.166	3.166

Table S2. The bond length and bond angle of S_8 and LiPSs in free states.

	S_8	Li_2S_8	Li_2S_6	Li_2S_4	Li_2S
S-S bond length(Å)	2.06	2.07	2.07	2.08	-
Li-S bond length(Å)	-	2.38	2.38	2.37	2.09
Li-Li bond length(Å)	-	2.57	2.66	2.80	-
Li-S-Li bond angle(°)	-	65.5	68.8)	73.3	111.8
S-S-S bond angle(°)	109	110.0	108.7	105.2	-
S- Li-S bond angle(°)	-	110.9	109.4	104.9	-

Table S3. The bond length and bond angle of S_8 and LiPSs adsorbed on the TiC(001) surface by the DFT-D3 method. The values in brackets are the corresponding information of the free species.

S_8	Li_2S_8	Li_2S_6	Li_2S_4	Li_2S
-------	-----------	-----------	-----------	---------

S-S bond length(Å)	2.07(2.06)	2.10(2.07)	2.11(2.07)	2.11(2.08)	-
Li-S bond length(Å)	-	2.63(2.38)	2.86(2.38)	2.80(2.37)	2.42(2.09)
Li-Li bond length (Å)		2.66(2.57)	2.79(2.66)	2.96(2.80)	
Ti-C bond length		2.21-2.19	2.22-2.17	2.22-2.17	
C-C bond length		3.10(3.06)	3.10(3.06)	3.10(3.06)	
Ti-Ti bond length		3.12(3.06)	3.12(3.06)	3.11(3.06)	
Li-S-Li bond angle(°)	-	63.9(65.5)	63.5(68.8)	70.0(73.3)	99.74(111.8)
S-S-S bond angle(°)	108.7(109)	107.4(110.0)	104.3(108.7)	106.3(105.2)	-
S- Li-S bond angle(°)	-	114.5(110.9)	115.8(109.4)	107.5(104.9)	-

Table S4. The bond length and bond angle of S_8 and LiPSs adsorbed on the VC(001) surface by the DFT-D3 method. The values in brackets are the corresponding information of the free species.

	S_8	Li_2S_8	Li_2S_6	Li_2S_4	Li_2S
S-S bond length(Å)	2.08(2.06)	2.10(2.07)	2.11(2.07)	2.11(2.08)	-
Li-S bond length(Å)	-	2.59(2.38)	2.67(2.38)	2.74(2.37)	2.20(2.09)
Li-Li bond length (Å)		2.70(2.57)	2.74(2.66)	3.04(2.80)	
V-C bond length		2.13-2.10	2.13-2.09	2.12-2.09	
C-C bond length		2.98(2.93)	2.98(2.93)	2.98(2.93)	
V-V bond length		3.00(2.93)	2.98(2.93)	2.98(2.93)	
Li-S-Li bond angle(°)	-	65.6(65.5)	63.5(68.8)	72.5(73.3)	90.17(111.8)
S-S-S bond angle(°)	108.6(109)	106.6(110.0)	103.2(108.7)	105.6(105.2)	-

S- Li-S bond angle(°)	-	113.5(110.9)	115.8(109.4)	105.5(104.9)	-
-----------------------	---	--------------	--------------	--------------	---

Table S5. The bond length and bond angle of S_8 and LiPSs adsorbed on the ZrC(001) surface by the DFT-D3 method. The values in brackets are the corresponding information of the free species.

	S_8	Li_2S_8	Li_2S_6	Li_2S_4	Li_2S
S-S bond length(Å)	2.08(2.06)	2.09(2.07)	2.11(2.07)	2.12(2.08)	-
Li-S bond length(Å)	-	2.80(2.38)	3.25(2.38)	3.15(2.35)	2.53(2.09)
Li-Li bond length (Å)		2.76(2.57)	3.03(2.66)	3.21(2.80)	
Zr-C bond length		2.40-2.38	2.41-2.36	2.42-2.36	
C-C bond length		3.36(3.33)	3.37(3.33)	3.38(3.33)	
Zr-Zr bond length		3.40(3.33)	3.38(3.33)	3.39(3.33)	
Li-S-Li bond angle(°)	-	63.4(65.5)	62.7(68.8)	69.5(73.3)	98.7(111.8)
S-S-S bond angle(°)	108.5(109)	107.1(110.0)	104.8(108.7)	108.3(105.2)	-
S- Li-S bond angle(°)	-	114.3(110.9)	115.8(109.4)	107.1(104.9)	-

Table S6. The bond length and bond angle of S_8 and LiPSs adsorbed on the NbC(001) surface by the DFT-D3 method. The values in brackets are the corresponding information of the free species.

	S_8	Li_2S_8	Li_2S_6	Li_2S_4	Li_2S
S-S bond length(Å)	2.09(2.06)	2.10(2.07)	2.11(2.07)	2.10(2.08)	-
Li-S bond length(Å)	-	2.64(2.38)	2.96(2.38)	3.05(2.35)	2.19(2.09)

Li-Li bond length (Å)		2.71(2.57)	2.9(2.66)	3.25(2.80)	
Nb-C bond length		2.31-2.28	2.30-2.25	2.28-2.26	
C-C bond length		3.22(3.18)	3.20(3.18)	3.23(3.18)	
Nb-Nb bond length		3.26(3.18)	3.22(3.18)	3.24(3.18)	
Li-S-Li bond angle(°)	-	65.2(65.5)	65.6(68.8)	71.8(73.3)	155.3(111.8)
S-S-S bond angle(°)	110.6(109)	106.1(110.0)	103.1(108.7)	106.8(105.2)	-
S- Li-S bond angle(°)	-	112.6(110.9)	113.3(109.4)	105.6(104.9)	-

Table S7. The bond length and bong angle of S_8 and LiPSs adsorbed on the HfC(001) surface by the DFT-D3 method. The values in brackets are the corresponding information of the free species.

	S_8	Li_2S_8	Li_2S_6	Li_2S_4	Li_2S
S-S bond length(Å)	2.08(2.06)	2.10(2.07)	2.12(2.07)	2.12(2.08)	-
Li-S bond length(Å)	-	2.76(2.38)	3.14(2.38)	3.09(2.35)	2.51(2.09)
Li-Li bond length (Å)		2.78(2.57)	2.99(2.66)	3.16(2.80)	
Hf-C bond length		2.37-2.35	2.38-2.33	2.39-2.33	
C-C bond length		3.33(3.28)	3.33(3.28)	3.34(3.28)	
Hf-Hf bond length		3.35(3.28)	3.34(3.28)	3.34(3.28)	
Li-S-Li bond angle(°)	-	64.8(65.5)	63.7(68.8)	69.62(73.3)	100.4(111.8)
S-S-S bond angle(°)	108.7(109)	106.9(110.0)	104.5(108.7)	107.6(105.2)	-
S- Li-S bond angle(°)	-	112.6(110.9)	114.7(109.4)	107.1(104.9)	-

Table S8. The bond length and bong angle of S_8 and LiPSs adsorbed on the TaC(001) surface by the DFT-D3 method. The values in brackets are the corresponding information of the free species.

	S_8	Li_2S_8	Li_2S_6	Li_2S_4	Li_2S
S-S bond length(Å)	20.7(2.06)	2.11(2.07)	2.12(2.07)	2.12(2.08)	-
Li-S bond length(Å)	-	2.65(2.38)	2.93(2.38)	3.09(2.35)	2.20(2.09)
Li-Li bond length (Å)		2.73(2.57)	2.92(2.66)	3.16(2.80)	
Ta-C bond length		2.29-2.27	2.30-2.25	2.29-2.26	
C-C bond length		3.20(3.16)	3.20(3.16)	3.20(3.16)	
Ta-Ta bond length		3.24(3.16)	3.22(3.16)	3.22(3.16)	
Li-S-Li bond angle(°)	-	65.7(65.5)	65.6(68.8)	72.47(73.3)	156.2(111.8)
S-S-S bond angle(°)	(110.2)109	105.1(110.0)	102.8(108.7)	106.6(105.2)	-
S- Li-S bond angle(°)	-	112.7(110.9)	113.3(109.4)	105.2(104.9)	-

Table S9. Bond Lengths of $Li_{1-C}(d_{Li1-C})$, $Li_{2-C}(d_{Li2-C})$, $S_{1-TM}(d_{S1-TM})$, and $S_{2-TM}(d_{S2-TM})$, and binding energies (E_b) for the adsorption of Li_2S_8 on the (001) facet of TMCs.

	E_{ads}	$d_{Li1-C}(\text{\AA})$	$d_{Li2-C}(\text{\AA})$	$d_{S1-TM}(\text{\AA})$	$d_{S2-TM}(\text{\AA})$
VC(001)	2.70	2.17	2.17	2.59	2.55
TiC(001)	2.81	2.18	2.17	2.62	2.61

TaC(001)	3.05	2.17	2.17	2.63	2.61
NbC(001)	3.04	2.17	2.18	2.69	2.67
HfC(001)	3.06	2.17	2.16	2.67	2.67
ZrC(001)	3.07	2.18	2.17	2.70	2.70

Table S10. Bond Lengths of Li1–C(d_{Li1-C}), Li2–C(d_{Li2-C}), S1–TM(d_{S1-TM}), and S2–TM(d_{S2-TM}), and binding energies (E_b) for the adsorption of Li_2S_6 on the (001) facet of TMCs.

	E_{ads}	$d_{Li1-C}(\text{\AA})$	$d_{Li2-C}(\text{\AA})$	$d_{S1-TM}(\text{\AA})$	$d_{S2-TM}(\text{\AA})$
VC(001)	2.41	2.17	2.21	2.57	2.63
TiC(001)	2.51	2.16	2.19	2.59	2.60
TaC(001)	2.69	2.15	2.13	2.63	2.64
NbC(001)	2.67	2.13	2.16	2.64	2.66
HfC(001)	2.71	2.16	2.18	2.65	2.65
ZrC(001)	2.71	2.18	2.20	2.67	2.68

Table S11. Bond Lengths of Li1–C(d_{Li1-C}), Li2–C(d_{Li2-C}), S1–TM(d_{S1-TM}), and S2–TM(d_{S2-TM}), and binding energies (E_b) for the adsorption of Li_2S_4 on the (001)

facet of TMCs.

	E_{das} (eV)	$d_{\text{Li1-C}}$ (Å)	$d_{\text{Li2-C}}$ (Å)	$d_{S1-\text{TM}}$ (Å)	$d_{S2-\text{TM}}$ (Å)
VC(001)	2.56	2.12	2.12	2.66	2.65
TiC(001)	2.66	2.11	2.12	2.68	2.67
TaC(001)	2.87	2.07	2.07	2.66	2.67
NbC(001)	2.85	2.09	2.09	2.69	2.69
HfC(001)	2.90	2.10	2.10	2.70	2.70
ZrC(001)	2.92	2.12	2.12	2.74	2.74

Table S12. The comparison of adsorption energy for the LiPSs on HfC(001) surface with or without DFT+U method.

	$E_{\text{ads}}\text{-Li}_2\text{S}_8/\text{eV}$	$E_{\text{ads}}\text{-Li}_2\text{S}_6/\text{eV}$	$E_{\text{ads}}\text{-Li}_2\text{S}_4/\text{eV}$
DFT	3.05	2.71	2.90
DFT+U (U=4 eV)	2.73	2.39	2.60

Table S13. The binding energies of Li_2S_8 , Li_2S_6 and Li_2S_4 with one and two organic molecules (i.e. DOL or DME).

	Li_2S_8	Li_2S_6	Li_2S_4
One DOL	0.81 eV	0.86 eV	0.82 eV
One DME	0.76 eV	0.74 eV	0.79 eV
Two DOL	1.81 eV	1.76 eV	1.77 eV

Two DME 1.58 eV 1.49 eV 1.56 eV

Table S14. The charge transfer (Δq , in e) of S or Li atoms in the S₈ or LiPSs adsorbed on TMCs.

	TiC	VC	ZrC	NbC	HfC	TaC
S ₈	-0.199	-0.114	-0.392	-0.391	-0.391	-0.119
Δ q (S)						
Li ₂ S ₈	-1.201	-1.146	-1.291	-1.248	-1.291	-1.262
Li ₂ S ₆	-1.164	-1.116	-1.258	-1.184	-1.252	-1.204
Li ₂ S ₄	-1.162	-1.058	-1.140	-1.136	-1.257	-1.146
Li ₂ S	-0.786	-1.165	-0.882	-1.246	-0.868	-1.126
Li ₂ S ₈	1.677	1.681	1.670	1.676	1.672	1.673
Δ q (Li)						
Li ₂ S ₆	1.694	1.695	1.692	1.692	1.690	1.690
Li ₂ S ₄	1.688	1.694	1.647	1.685	1.678	1.685
Li ₂ S	1.706	1.702	1.687	1.685	1.690	1.685

Table S15. The detailed test data of Li ions adsorbed on the (001) surfaces of TMCs.

	Initial adsorption site	Bri	Top-TM	Top-C	Hollow
TiC (001) surface	Final adsorption site	Top-C	Top-Ti	Top-C	Top-C
	E _{ads} (eV)	2.24	1.62	2.24	2.24
VC (001) surface	Final adsorption site	Top-C	Top-V	Top-C	Top-C
	E _{ads} (eV)	2.09	1.53	2.09	2.09
ZrC (001) surface	Final adsorption site	Top-C	Top-Zr	Top-C	Top-C
	E _{ads} (eV)	2.08	1.04	2.08	2.08
NbC (001) surface	Final adsorption site	Top-C	Top-Nb	Top-C	Top-C

	E_{ads} (eV)	1.74	0.95	1.74	1.74
HfC (001) surface	Final adsorption site	Top-C	Top-Hf	Top-C	Top-C
	E_{ads} (eV)	1.99	0.99	1.99	1.99
TaC (001) surface	Final adsorption site	Top-C	Top-Ta	Top-C	Top-C
	E_{ads} (eV)	1.64	0.93	1.64	1.64

References:

- [1] J. Mao, S. Li, Y. Zhang, X. Chu, Z. Yang, The stability of TiC surfaces in the environment with various carbon chemical potential and surface defects, *Applied Surface Science*, 386 (2016) 202-209.
- [2] C. Kunkel, F. Viñes, P.J. Ramírez, J.A. Rodriguez, F. Illas, Combining Theory and Experiment for Multitechnique Characterization of Activated CO₂ on Transition Metal Carbide (001) Surfaces, *The Journal of Physical Chemistry C*, 123 (2019) 7567-7576.
- [3] S.N. Lekakh, N.I. Medvedeva, Ab initio study of Fe adsorption on the (001) surface of transition metal carbides and nitrides, *Computational Materials Science*, 106 (2015) 149-154.
- [4] H. Prats, M. Stamatakis, Atomistic and electronic structure of metal clusters supported on transition metal carbides: implications for catalysis, *Journal of Materials Chemistry A*, 10 (2022) 1522-1534.
- [5] R. Dronskowski, P.E. Bloechl, Crystal orbital Hamilton populations (COHP): energy-resolved visualization of chemical bonding in solids based on density-functional calculations, *The Journal of Physical Chemistry*, 97 (1993) 8617-8624.
- [6] R. Nelson, C. Ertural, J. George, V.L. Deringer, G. Hautier, R. Dronskowski, LOBSTER: Local orbital projections, atomic charges, and chemical-bonding analysis from projector-augmented-wave-based density-functional theory, *J Comput Chem*, 41 (2020) 1931-1940.
- [7] W. Lv, J. Deng, D. Wu, B. He, G. Tang, D. Ma, Y. Jia, P. Lv, Similar electronic state effect enables excellent activity for nitrate-to-ammonia electroreduction on both high- and low-density double-atom catalysts, *The Journal of Chemical Physics*, 159 (2023).
- [8] P. Lv, W. Lv, D. Wu, G. Tang, X. Yan, Z. Lu, D. Ma, Ultrahigh-Density Double-Atom Catalyst with Spin Moment as an Activity Descriptor for the Oxygen-Reduction Reaction, *Physical Review Applied*, 19 (2023) 054094.
- [9] R. Jayan, M.M. Islam, Mechanistic Insights into Interactions of Polysulfides at VS₂ Interfaces in Na-S Batteries: A DFT Study, *ACS Applied Materials & Interfaces*, 13 (2021) 35848-35855.
- [10] X. Song, Y. Qu, L. Zhao, M. Zhao, Monolayer Fe₃GeX₂ (X = S, Se, and Te) as Highly Efficient Electrocatalysts for Lithium–Sulfur Batteries, *ACS Applied Materials & Interfaces*, 13 (2021) 11845-11851.